REGIONAL GEOLOGICAL CONTEXT OF THE INSIGHT LANDING SITE FROM MINERALOGY AND STRATIGRAPHY. L. Pan[1] and C. Quantin[1], [1]Laboratoire de Géologie de Lyon, Université Claude Bernard Lyon 1 (2 rue Raphaël Dubois, Bâtiment GEODE, Villeurbanne, 69622. lu.pan@univ-lyon1.fr).

Introduction: Planned to launch in May 2018, the InSight (Interior Exploration using Seismic Investigations, Geodesy and Heat Transport) robotic lander will explore the interior of Mars with a set of geophysical instruments [1-2]. Orbital data for the InSight landing site may provide crucial information on the regional context, rock properties and potential structural discontinuities in the crust, which can be utilized to better interpret the future seismic data collected by SEIS (Seismic Experiment for Interior Structures) instrument on board InSight lander. Complementary to the previous studies on the surface properties in the landing ellipses [3-4], here we present a study on the regional geologic context of the landing site using a combination of orbital datasets and discuss the interpretation for the lithology and structure in the subsurface of the landing site.

Geologic context: Situated between the Elysium volcanic structure and the dichotomy boundary, the InSight landing site region has been shaped by the early formation and subsequent modification of the Martian dichotomy. The landing site is situated in an Early Hesperian transition unit [5-6], inferred to be volcanic in origin [3], overlain by the Elysium Mons volcanic unit [7] and younger lavas from Cerberus Fossae [5,7] to the north and the Medusae Fossae Formation to the east [8].

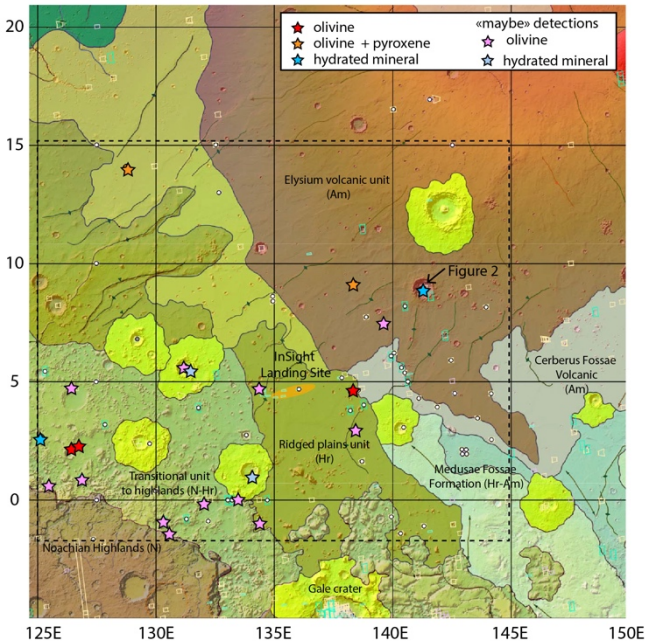

Figure 1: Geological map of the InSight landing site vicinity based on [6], with major geological units labeled and inferred age of each unit given in brackets (Am: Amazonian, Hr: Hesperian, N: Noachian). Stars show the mineral detections from CRISM data.

The surface of the landing site is covered by >3 m thick regolith, evidenced by the onset diameter of small rocky ejecta craters [4]. As a consequence, this investigation is focused on the limited exposures in the craters and local scarps in this region.

Method: We analyzed 79 CRISM (Compact Reconnaissance Imaging Spectrometer for Mars) targeted images (18-36 m/pixel, 438 channels) in the landing site region (125°E to 145°E, 2°S to 15°N), following the data processing method in the previous northern lowlands survey [9]. For locations where subsurface mineralogy is detected, we analyzed the accompanying HiRISE (High Resolution Imaging Science Experiment) and CTX (Context Camera) images to investigate the correlation of the mineral detections with morphological units. The annual median thermal inertia of relevant units is derived from measurements by the Thermal Emission Spectrometer [10].

Results: *Mafic detections in the volcanic units.* Olivine spectral signatures with weak absorptions are detected on small craters rims close to the landing site, on the ridged plains unit (Fig. 1). The mineral detection is well-correlated with the bedrock exposure on the crater wall. The olivine-rich composition; surface expression of wrinkle ridges and the relatively older age compared to nearby volcanic units [5-6] imply their relation to the Hesperian lava flow units widespread in the northern lowlands [11-13]. Both olivine and low-calcium pyroxene are found in a small crater within the Elysium Mons unit to the north of the landing ellipse, indicating either a different composition or heavier dust cover masking pyroxene absorptions in the ridged plains unit. More definitive olivine and clay detections are found in the transitional unit close to the dichotomy, which could be the remnants of highlands materials, possibly of similar origin as the adjacent stratigraphy in the Sharp-Knobel watershed [14].

Phyllosilicate detection and layered unit in a 50-km crater. Of particular interest is the Fe/Mg phyllosilicate identified in the central peak of a 50-km crater on the southwest flank of Elysium Mons. The phyllosilicate detection based on the 2.3 and 1.9 μm bands show the strongest absorptions in a topographic depression within the central peak. Similar spectral features with weaker absorptions are found in the adjacent central peak, which consists of a fragmented unit characterized by relatively light-toned features and heavily eroded morphology (Fig. 2C-D). The alternating resistant (cliff-forming) and friable (slope-forming) layers in this unit form an irregular cliff-bench morphology, exhibiting

extensive layering of <10 m thick. The fragments of 2-5 meters in size within the unit show evidence of little to no relative displacement (Fig. 2E).

Discussion: *Possible origins of layered units.* The clay-bearing unit in the central peak of a 50-km crater in the Elysium volcanic unit, is found with light-toned, cliff-bench morphology, consistent with the attributes of sedimentary rocks identified elsewhere on Mars [15]. Though the morphology resembles certain locations in the lower member of the Medusae Fossae Formation [16], the unit has distinctively higher thermal inertia (up to 500-1000 J m^{-2} K^{-1} $s^{-½}$) than that of the Medusae Fossae Formation.

The feature of incipient fracturing (Fig. 2E) in the layers suggests they likely result from the structural uplift of a homogeneous rock mass at the impact event, instead of deposition at a later stage. The original depth of the central peak unit is >3-4 km, inferred from the size of the impact crater. Such layering units may form via subaerial (aeolian, volcaniclastic) or subaqueous processes before the emplacement of Elysium Mons lavas. The detection of Fe/Mg phyllosilicates associated with the central peak indicates aqueous alteration has occurred, which may be directly related to the presence of water during deposition. Alternatively, the layering structure and fragmentation in the unit could make it more susceptible to alteration after its deposition or excavation by the impact. Though the exposure is limited, it is possible that such unit is more extensive within the subsurface of Elysium Planita. Other large craters in the landing site vicinity also show possible detections of hydrated minerals, but the absorptions are obscured, likely due to a combination of noise and dust mixing.

Inferred stratigraphy and implications for InSight. The overall stratigraphy of the landing site shows a gradational sequence which becomes younger toward Elysium Mons. This analysis suggests a clay-bearing sedimentary unit underlies lava flows of several kilometers thick and a regolith layer close to the InSight landing site. The presence of these different geologic units in the subsurface of the landing site can result in variations in density or seismic anisotropy, which may be analyzed using data collected by the seismic instrument on board InSight lander.

Future work: To better understand the origin of the layered unit, further analysis will focus on its distribution and the thickness and orientation of the layers through continued survey of HiRISE images and digital elevation models. We will also extend the investigation to regions around Elysium Mons and the adjacent highland crust, to gain a wider view of crustal structure and geologic history of the InSight landing site vicinity.

Acknowledgement: This project has received funding from the European Union's Horizon 2020 research and innovation programme under the Marie Sklodowska-Curie grant agreement No. 751164.

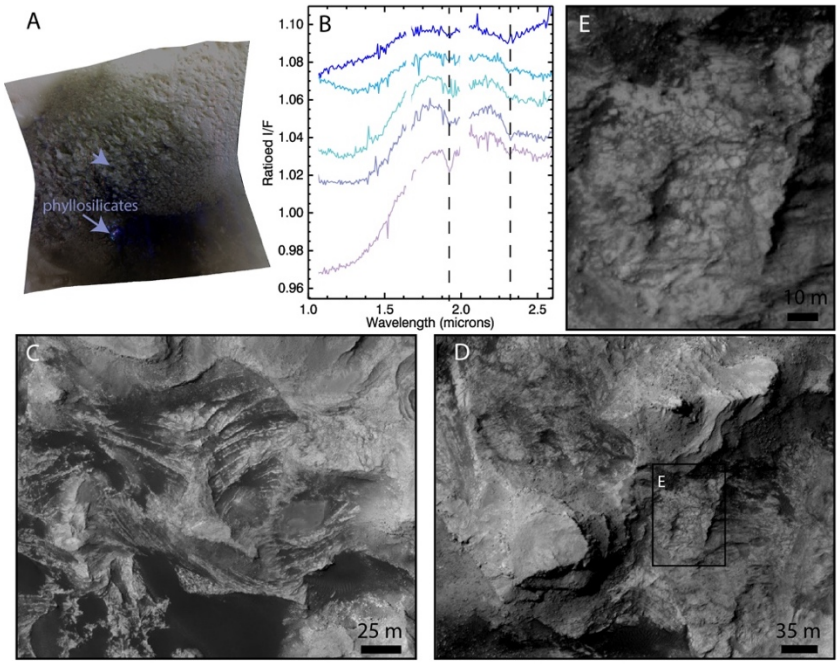

Figure 2: Layered units wi th phyllosilicates in unnamed large crater central peak. A. CRISM false color image overlain by spectral parameter map highlighting phyllosilicate detections. B. Type spectra of phyllosilicate detections in the central peak. C-D. Cliff-bench morphology of the central peak layered unit. E. Details of the fragmentation of the layered unit.

References: [1] Banerdt W.B. et al. (2013) *LPS XLV* Abstract #1915. [2] Banerdt W. B. *et al.* (2017) *LPS XLVIII* Abstract #1896. [3] Golombek M., et al. (2017) *Space Sci. Rev.* 211, 1-4, 5-95. [4] Warner N. H. *et al. Space Sci. Rev. 211,* 1-4, 147-190. [5] Tanaka K. L., Chapman M. G. and Scott D. H. (1992) *USGS* No. 2147. [6] Tanaka K. L. et al. (2014) *Planet. Space Sci* 95, 11-24. [7] Vaucher J. et al. (2009) *Icarus* 204, 2, 418-422. [8] Kerber L. and Head J. W. (2010) *Icarus* 206, 2: 669-684. [9] Pan et al. (2017) *JGR Planets*, 122, 9, 1824-1854. [10] Putzig et al. (2013) *AGU*. [11] Head J. W., Kreslavsky M. A. and Pratt S. (2002) *JGR Planets* 107, E1. [12] Salvatore M. R. *et al.* (2010). *JGR Planets*, 115(E7). [13] Ody, A. *et al.* (2013) *JGR Planets* 118, 2: 234-262. [14] Ehlmann, B. L. and Buz J. (2015) *GRL* 42, 2, 264-273. [15] Malin, M. C. and Edgett K. S. (2000) *Science* 290, 5498, 1927-1937. [16] Zimbelman J. R. and Griffin L. J. (2010) *Icarus* 205, 1, 198-210.